Available online at www.sciencedirect.com
ScienceDirect
Journal of Sound and Vibration 301 (2007) 429–449
JOURNAL OF SOUND AND VIBRATION
www.elsevier.com/locate/jsvi

Active vibration control of structural systems by a combination of the linear quadratic Gaussian and input estimation approaches

Chih-Chergn Ho[a], Chih-Kao Ma[b,*]

[a]Department of System Engineering, Chung-Cheng Institute of Technology, Ta-Hsi Taoyuan, 335, Taiwan, Republic of China
[b]Department of Naval Architecture and Marine Engineering, Chung-Cheng Institute of Technology, Ta-Hsi Taoyuan, 335, Taiwan, Republic of China

Received 5 November 2003; received in revised form 25 June 2004; accepted 22 December 2005
Available online 16 January 2007

Abstract

This study proposes an active control method to suppress the responses of structural systems. The present control method is a synthesis algorithm of the linear quadratic Gaussian (LQG) and input estimation approaches. By using the synthesis method, structural vibrations can be suppressed more effectively due to the actions of the proper control forces. In this work, numerical simulations of active vibration control of lumped-mass systems are performed to verify the feasibility and effectiveness of the proposed algorithm. The simulation results demonstrate that the control performance of the present method for structures with external excitation forces is better than that of the conventional LQG approach.

1. Introduction

For the design of structural systems, to make the structures have a desired transient and steady-state response is a very important and necessary task. In terms of passive control methods, the unwanted vibration problems can be solved effectively. However, for some physical systems, the structural parameters such as mass, damping and stiffness cannot be chosen or changed to make the responses satisfy the requirements because of design constraints. Therefore, many active control methods are developed by using external adjustable or active devices to shape or control the responses. Comparing with passive control methods, active control methods can suppress the structural vibration more effectively under various conditions.

Among the active vibration control methods, optimal control methods, such as linear quadratic regulator (LQR) and LQG, are popular with many structural engineers. Yang [1] applied the optimal control theorem to control the vibrations of civil engineering structures under stochastic dynamic loadings such as earthquakes and wind loads. Chung et al. [2,3] presented an experimental study of active control for single degree-of-freedom (sdof) and multiple degree-of-freedom (mdof) seismic structures by using tendons through an optimal

*Corresponding author. Tel.: +886 3 380 0958; fax: +886 3 389 2134.
E-mail address: chihkao@ccit.edu.tw (C.-K. Ma).

0022-460X/$ - see front matter
doi:10.1016/j.jsv.2005.12.061

Nomenclature

A	constant matrix
B	constant matrix
D	constant matrix
G	constant matrix
B_s	sensitivity matrices
C	damping matrix
F	input force vector (the unknown inputs to be estimated)
U	control force vector
H	measurement matrix
I	identity matrix
k	time (discretized)
K	stiffness matrix
K_a	Kalman gain
K_b	correction gain
K_r	regulator gain
K_∞	regular gain of infinite horizon
M	mass matrix
M_s	sensitivity matrices
P	filter's error covariance matrix
P_b	error covariance matrix
Q	process noise covariance matrix
Q_s	scalar of process noise covariance
R	measurement noise covariance matrix
R_v	measurement noise covariance
S	innovation covariance
Q_0	weighting matrix for the final state
Q_1	weighting matrix for the response
Q_2	weighting matrix for the control force
Q_s	state weighting
Q_c	control weighting
t	time (continuous)
v	measurement noise vector
w	process noise vector
X	state vector
Y	relative displacement vector
$\dot{Y}$	relative velocity vector
$\ddot{Y}$	relative acceleration vector
Z	observation vector
γ	fading factor
Γ	input matrix
δ	Kronecker delta
ΔT	sampling time
Δt	incremental time
σ	standard deviation
Φ	state transition matrix
y	relative displacement
$\dot{y}$	relative velocity
$\ddot{y}$	relative acceleration
m	mass
k	stiffness constant of the linear term
c	damping constant of the linear term
$a(t)$	absolute acceleration of the base motion

Superscripts

$\hat{}$	estimated
–	estimated by filter
T	transpose of matrix
*	nominal

Subscripts

i, j	indices

closed-loop control scheme. They also presented the optimal direct output feedback and acceleration feedback control algorithms for seismic structures [4–6]. Yang et al. [7] used the instantaneous optimal control method, which minimizes the quadratic performance index at every time instant, to overcome the deficiency of neglecting the earthquake input. An experimental work to verify the control method was also presented [8]. Loh et al. [9] conducted an active structural control experiment to verify the current state-of-the-art control algorithm by using a full-scale building with active bracing devices. Chang and Yu [10] proposed a simple pole placement technique for the control of a structural system subjected to a white noise ground excitation. Recently, Xu and Yang [11] applied the dominant internal model approach to implement the predictive control of structural responses to external excitations. Akhiev et al. [12] used the multipoint performance index for the vibration suppression of earthquake-excited structures.

In all of the above-mentioned references, the control algorithms can be grouped into two types, one ignoring the input excitations term, and the other considering that. For the latter type, the input excitations need to be measurable or the class of the disturbances has to be known. However, many physical structural systems in fact contain arbitrary, unmeasurable excitation forces. Hence, the object

of this study is to develop a method using the quadratic optimal control that involves considering the arbitrary external loadings or unmeasurable disturbances in the calculation of control forces. The method consists of the LQG and input estimation approaches [13]. The input estimation approach has been successfully used to identify input forces for structural systems [14,15]. In this study, the negative values of estimated input forces are added into the control forces evaluated by LQG regulator to eliminate the external loadings.

This paper first briefly reviews the equations of motion of lumped-mass structural systems subjected by seismic excitations. A synthesis control algorithm of suppressing the structural vibrations is then developed. The control method is composed of the LQG regulator and input estimation approach. The feasibility of the proposed method is verified by numerical simulations of active vibration controls for the lumped-mass systems. The dynamic responses of structural systems are obtained by Newmark's β method. The proposed algorithm then uses the responses to simulate the measurements of the observer. From the control results of the lumped-mass structures, we can conclude that the proposed algorithm can suppress structural vibrations more effectively and is better than the conventional LQG approach.

2. Modeling of the structural system

2.1. Equations of motion

For a dof lumped-mass structural system under active control, as shown in Fig. 1(a), the equations of motion can be written as below:

$$M\ddot{Y}(t) + C\dot{Y}(t) + KY(t) = F(t) + DU(t), \tag{1}$$

where M denotes the $n \times n$ mass matrix, C the $n \times n$ damping matrix, K the $n \times n$ stiffness matrix, D the $n \times n$ control force distribution matrix, $F(t)$ the $n \times 1$ input force vector, $U(t)$ the $n \times 1$ control force vector, and $\ddot{Y}$, $\dot{Y}$, Y the $n \times 1$ vectors of relative acceleration, velocity and displacement, respectively; and

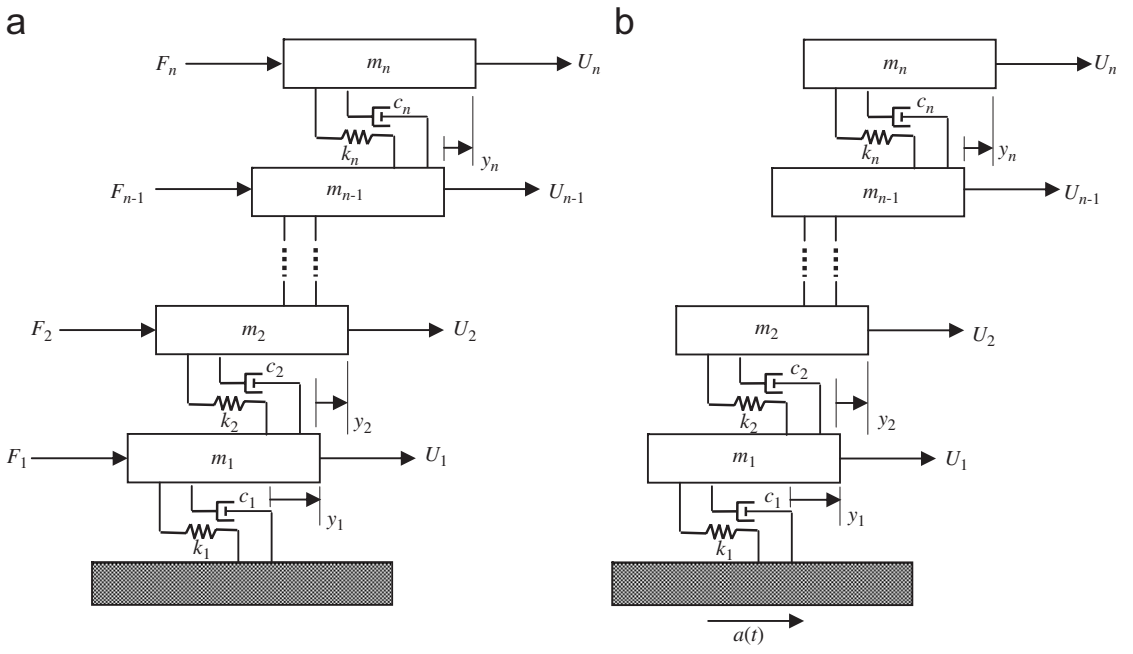

Fig. 1. A mdof lumped-mass structure (a) under force excitation, and (b) under seismic excitation.

$$M = \begin{bmatrix} m_1 & 0 & 0 & \cdots & 0 \\ m_2 & m_2 & 0 & \cdots & 0 \\ m_3 & m_3 & m_3 & \cdots & 0 \\ \vdots & \vdots & \vdots & \ddots & \vdots \\ m_n & m_n & m_n & \cdots & m_n \end{bmatrix}_{n\times n},$$

$$C = \begin{bmatrix} c_1 & -c_2 & 0 & 0 & \cdots & 0 & 0 \\ 0 & c_2 & -c_3 & 0 & \cdots & 0 & 0 \\ 0 & 0 & c_3 & -c_4 & \cdots & 0 & 0 \\ \vdots & \vdots & \ddots & \ddots & \ddots & \vdots & \vdots \\ 0 & 0 & 0 & \ddots & \ddots & -c_{n-1} & 0 \\ 0 & 0 & 0 & \cdots & \ddots & c_{n-1} & -c_n \\ 0 & 0 & 0 & \cdots & \cdots & 0 & c_n \end{bmatrix}_{n\times n},$$

$$K = \begin{bmatrix} k_1 & -k_2 & 0 & 0 & \cdots & 0 & 0 \\ 0 & k_2 & -k_3 & 0 & \cdots & 0 & 0 \\ 0 & 0 & k_3 & -k_4 & \cdots & 0 & 0 \\ \vdots & \vdots & \ddots & \ddots & \ddots & \vdots & \vdots \\ 0 & 0 & 0 & \ddots & \ddots & -k_{n-1} & 0 \\ 0 & 0 & 0 & \cdots & \ddots & k_{n-1} & -k_n \\ 0 & 0 & 0 & \cdots & \cdots & 0 & k_n \end{bmatrix}_{n\times n},$$

$$\ddot{Y} = \begin{bmatrix} \ddot{y}_1 \\ \ddot{y}_2 \\ \vdots \\ \ddot{y}_n \end{bmatrix}_{n\times 1}, \quad \dot{Y} = \begin{bmatrix} \dot{y}_1 \\ \dot{y}_2 \\ \vdots \\ \dot{y}_n \end{bmatrix}_{n\times 1}, \quad Y = \begin{bmatrix} y_1 \\ y_2 \\ \vdots \\ y_n \end{bmatrix}_{n\times 1}, \quad F = \begin{bmatrix} F_1 \\ F_2 \\ \vdots \\ F_n \end{bmatrix}_{n\times 1}, \quad U = \begin{bmatrix} U_1 \\ U_2 \\ \vdots \\ U_n \end{bmatrix}_{n\times 1}.$$

In order to investigate structures with a base motion excitation, we also consider an mdof structural system subjected to an earthquake ground motion, as shown in Fig. 1(b). The input forces, i.e., external applied forces, in Eq. (1) are replaced by the mass times the acceleration vector. It follows that

$$M\ddot{Y}(t) + C\dot{Y}(t) + K(t)Y(t) = -M[\bar{1}]a(t) + DU(t), \tag{2}$$

where $[\bar{1}]$ is a $n \times 1$ column vector whose first element is one, the other elements are all to be zeros and $a(t)$ is the absolute acceleration of the base motion or ground motion. In fact, Eq. (2) can be regarded as a special case of Eq. (1).

2.2. Evaluation of dynamic responses

The Newmark's β method is used to predict the responses of linear lumped-mass structures acted by dynamic loadings and control forces. Considering the simplicity and efficiency, we adopt the constant average acceleration method (i.e., $\beta = \frac{1}{4}$). The method is a forward integration in time domain and unconditionally

stable. In terms of the incremental equations of motion, the responses of the controlled structures at every time step can be computed as follows [16]:

$$K_D = K + \frac{2}{\Delta t} C + \frac{4}{\Delta t^2} M, \tag{3}$$

$$F_D = \Delta F + \Delta U + 2C\,\dot{Y}(t) + M\frac{4}{\Delta t}\,\dot{Y}(t) + M2\,\ddot{Y}(t), \tag{4}$$

$$\Delta Y = K_D^{-1} F_D, \tag{5}$$

$$Y(t + \Delta t) = Y(t) + \Delta Y, \tag{6}$$

$$\dot{Y}(t + \Delta t) = \frac{2}{\Delta t}\Delta Y - \dot{Y}(t), \tag{7}$$

$$\ddot{Y}(t + \Delta t) = \frac{4}{\Delta t^2}\Delta Y - \frac{4}{\Delta t}\,\dot{Y}(t) - \ddot{Y}(t), \tag{8}$$

where K_D, F_D, ΔF, ΔU, ΔY, Δt are dynamic stiffness matrix, equivalent dynamic load matrix, incremental input force matrix, incremental control force matrix, incremental displacement matrix and incremental time, respectively. In this study, the white noises, which were assumed to be the pseudo process and measurement noises, were added into the input forces and simulated pure responses of Eq. (1). The simulated dynamic responses corrupted by the pseudo process and measurement noises are used to simulate the real measured responses.

2.3. State space model of the system

To apply the input estimation approach and LQG theory to structural systems, we first transform the equations of motion into the state equations. The transformation can be achieved by selecting the state vector $X(t) = [Y(t), \dot{Y}(t)]^{\mathrm{T}}$. According to Eq. (1), the continuous-time state and measurement equations can be written as

$$\dot{X}(t) = A\,X(t) + B\,F(t) + GU(t), \tag{9}$$

$$Z(t) = H\,X(t), \tag{10}$$

where

$$A(t) = \begin{bmatrix} 0_{n\times n} & I_{n\times n} \\ -M^{-1}K & -M^{-1}C \end{bmatrix}, \quad B = \begin{bmatrix} 0_{n\times n} \\ M^{-1} \end{bmatrix}, \quad G = \begin{bmatrix} 0_{n\times n} \\ M^{-1}D \end{bmatrix},$$

$$H = \begin{bmatrix} I_{n\times n} & 0_{n\times n} \end{bmatrix},$$

$$X(t) = \begin{bmatrix} x_1(t) & x_2(t) & \cdots & x_{2n-1}(t) & x_{2n}(t) \end{bmatrix}^{\mathrm{T}}.$$

$$F(t) = \begin{bmatrix} F_1(t) & F_2(t) & \cdots & F_{n-1}(t) & F_n(t) \end{bmatrix}^{\mathrm{T}}.$$

Next, the continuous state and measurement equations are discretized over time intervals of length ΔT. Considering the uncertainties and disturbances in the real physical world, the input process and measurement noises are added into the discretized state and measurement equations, respectively. The discrete-time forms of the state and measurement equations are shown as follows:

$$X(k) = \Phi\,X(k-1) + \Gamma\,(F(k-1) + w(k-1)) + \Lambda\,U(k-1), \tag{11}$$

$$Z(k) = H\,X(k) + v(k), \tag{12}$$

where

$$\Phi = \exp(A\,\Delta T),$$

$$\Gamma = \int_{(k-1)\Delta T}^{k\Delta T} \exp[A(k\Delta T - \tau)]B\,\mathrm{d}\tau,$$

$$\Lambda = \int_{(k-1)\Delta T}^{k\Delta T} \exp[A(k\Delta T - \tau)]G\,\mathrm{d}\tau,$$

$$H = \begin{bmatrix} I_{n\times n} & 0_{n\times n} \end{bmatrix},$$

$$F(k-1) = \begin{bmatrix} F_1(k-1) & F_2(k-1) & \cdots & F_{n-1}(k-1) & F_n(k-1) \end{bmatrix},$$

$$Z(k) = \begin{bmatrix} z_1(k) & z_2(k) & \cdots & z_{n-1}(k) & z_n(k) \end{bmatrix},$$

$$w(k) = \begin{bmatrix} w_1(k) & w_2(k) & \cdots & w_{n-1}(k) & w_n(k) \end{bmatrix},$$

$$v(k) = \begin{bmatrix} v_1(k) & v_2(k) & \cdots & v_{n-1}(k) & v_n(k) \end{bmatrix},$$

where $X(k)$ is the state vector, $F(k)$ the sequence of deterministic input, ΔT sampling time interval, $Z(k)$ the observation vector. The process noise vector $w(k)$ is assumed to be zero mean and white with variance $E\{w(k)\,w(j)^{\mathrm{T}}\} = Q\delta_{kj}$. Here, δ_{kj} is the Kronecker delta. The measurement noise vector $v(k)$ is also assumed to be zero mean and white. The variance of $v(k)$ is given by $E\{v(k)\,v(j)^{\mathrm{T}}\} = R\delta_{kj}$. Here, $R = \sigma^2$ and σ represents the standard deviation of the measurement noise. The matrices Φ, Γ, Λ, and H are the state transition matrix, input matrix, control matrix, and measurement matrix, respectively.

3. Control algorithm

3.1. The recursive input estimation approach

In the previous section, the discrete-time state equations of a linear mdof lumped-mass system subjected to dynamic loads and control forces have been derived. The magnitudes of the unknown input loads can be estimated by an inverse method from the noisy measurements of the system responses. For linear structural systems, the estimation method consists of two parts; one is the Kalman filter [17,18] with control but no input terms and the other is a recursive least-squares estimator. The recursive least-squares estimator is derived to compute the onset time histories of the unknown input loads by utilizing the Kalman gain, residual innovation covariance, and residual innovation generated by the Kalman filter. The detailed derivation and explanation of this technique can be found in Tuan et al. [13].

The equations of the Kalman filter with control but no input terms are

$$\bar{X}(k/k-1) = \Phi\bar{X}(k-1/k-1) + \Lambda U(k-1), \tag{13}$$

$$P(k/k-1) = \Phi P(k-1/k-1)\Phi^{\mathrm{T}} + \Gamma Q\Gamma^{\mathrm{T}}, \tag{14}$$

$$\bar{Z}(k) = Z(k) - H[\Phi\bar{X}(k-1/k-1) + \Lambda U(k-1)], \tag{15}$$

$$S(k) = HP(k/k-1)H^{\mathrm{T}} + R, \tag{16}$$

$$K_a(k) = P(k/k-1)H^{\mathrm{T}}S^{-1}(k), \tag{17}$$

$$P(k/k) = [I - K_a(k)H]P(k/k-1), \tag{18}$$

$$\bar{X}(k/k) = \Phi\bar{X}(k/k-1) + K_a(k)\bar{Z}(k). \tag{19}$$

The equations of the recursive least-squares estimator are

$$B_s(k) = H[\Phi M_s(k-1) + I]\Gamma, \tag{20}$$

$$M_s(k) = [I - K_a(k)H][\Phi M_s(k-1) + I], \tag{21}$$

$$K_b(k) = \gamma^{-1}(k)P_b(k)B_s^{\mathrm{T}}(k)\left[\gamma^{-1}(k)B_s(k)P_b(k-1)B_s^{\mathrm{T}}(k) + S(k)\right]^{-1}, \tag{22}$$

$$P_b(k) = \gamma^{-1}(k)[I - K_b(k)B_s(k)]P_b(k-1), \tag{23}$$

$$\hat{F}(k) = \hat{F}(k-1) + K_b(k)\left[\bar{Z}(k) - B_s(k)\hat{F}(k-1)\right], \tag{24}$$

where P is the filter's error covariance matrix, $S(k)$ the innovation covariance, $K_a(k)$ Kalman gain, $B_s(k)$ and $M_s(k)$ the sensitivity matrices, $\bar{Z}(k)$ the innovation, $K_b(k)$ the correction gain for updating $\hat{F}(k)$, $P_b(k)$ the error covariance of the estimated input vector, and $\hat{F}(k)$ the estimated input vector. The fading factor $\gamma(k)$ is employed to compromise between the fast tracking capability and the loss of estimate accuracy. In this study, the adaptive weighting method developed in Tuan and Hou [19] is used to select a suitable $\gamma(k)$. That is,

$$\gamma(K) = \begin{cases} 1, & \left|\bar{Z}(k)\right| \leqslant \sigma, \\ \sigma/|\bar{Z}(k)|, & \left|\bar{Z}(k)\right| > \sigma. \end{cases} \tag{25}$$

Thus, the computational procedure for the estimation of input forces acting on linear lumped-mass systems is summarized as follows:

Step 1: Derive the dynamic equations (Eqs. (11) and (12)) and obtain the simulated responses $Z(k)$ by Newmark's β method, i.e., Eqs. (3)–(8).
Step 2: Use the Kalman filter equations, i.e., Eqs. (13)–(19), to generate the innovation covariance $S(k)$, innovation $\bar{Z}(k)$, and Kalman gain $K_a(k)$.
Step 3: Use the recursive least-squares estimator, i.e., Eqs. (20)–(24), to compute the unknown input disturbance forces $\hat{F}(k)$.

3.2. LQG controller [20]

For standard linear quadratic Gaussian problems, the system under control is assumed to be described by the stochastic discrete-time state space equations as below

$$X(k) = \Phi\, X(k-1) + \Lambda\, U(k-1) + \Gamma\, w(k-1), \tag{26}$$

$$Z(k) = H\, X(k) + v(k), \tag{27}$$

where $w(k)$ and $v(k)$ are zero-mean white noises with variances Q and R, respectively. In general, the input forces sequence $F(k)$ are neglected or assumed to be zeros in conventional LQG design. The conventional LQG method is used to find $U(k)$ as a function of $X(k)$, $i \leqslant k \leqslant N-1$, so as to minimize the performance index

$$J_i(U) = E\left\{\frac{1}{2}X^{\mathrm{T}}(N)Q_0X(N) + \frac{1}{2}\sum_{k=i}^{N-1}\left[X^{\mathrm{T}}(k)Q_1X(k) + U^{\mathrm{T}}(k)Q_2(k)U(k)\right]\right\}, \tag{28}$$

where $Q_1 \geqslant 0$, $Q_2 > 0$, and $Q_0 \geqslant 0$ are all symmetric weighting matrices.

The separation theorem [21] provides the optimal feedback control law

$$U(k) = -K_r(k)\,\hat{X}(k). \tag{29}$$

Here $\hat{X}(k)$ is the state vector estimated by the Kalman filter, i.e., Eqs. (13)–(19). In other words, $\hat{X}(k)$ is equal to $\bar{X}(k)$ here because of no input forces term in Eq. (26). The regular gain $K_r(k)$ is given by

$$K_r(k) = \left[\Lambda^{\mathrm{T}}P_2(k+1)\Lambda + Q_2\right]^{-1}\Lambda^{\mathrm{T}}P_2(k+1)\Phi, \tag{30}$$

where $P_2(k)$ is the solution of the Ricatti equation

$$P_2(k) = \Phi^{\mathrm{T}}\left\{P_2(k+1) - P_2(k+1)\Lambda\left[\Lambda^{\mathrm{T}}P_2(k+1)\Lambda + Q_2\right]^{-1}\Lambda^{\mathrm{T}}P_2(k+1)\right\}\Phi + Q_1, \quad k \leqslant N, \tag{31}$$

$$P_2(N) = Q_0.$$

If the limiting solution to the Ricatti equation exists and is denoted by $P_2(\infty)$, then the corresponding steady-state regulator gain, which is a constant feedback gain, is

$$K_\infty = \left[\Lambda^{\mathrm{T}}P_2(\infty)\Lambda + Q_2\right]^{-1}\Lambda^{\mathrm{T}}P_2(\infty)\Phi. \tag{32}$$

3.3. Combination of the LQG and input estimation approaches

In the previous section, the LQG control methodology for a system without input forces term was discussed. The system, e.g. Eq. (26), is not satisfactory to model most dynamic structures because there usually exist external exciting forces. Therefore, we considered the case where the input forces were not zeros, i.e., Eqs. (11) and (12). However, the conventional LQG control methodology is not applicable to structures without neglecting the input disturbance forces, because the entire input dynamic loads histories are not known a priori.

Hence, we propose a synthesis method for structural vibration control considering the input disturbance forces. The proposed method is the combination of the LQG and input estimation approaches. The input estimation approach is introduced to observe the input disturbance forces for the open loop control, which is used to cancel out the input forces. By combining the open loop and LQG feedback control laws, the synthesis control method is established as follows:

$$U(k) = -K_r(k)\,\hat{X}(k) - (\Lambda^{\mathrm{T}}\Lambda)^{-1}\Lambda^{\mathrm{T}}\,\Gamma\,\hat{F}(k). \tag{33}$$

Here $\hat{X}(k)$ is the state vector estimated by the Kalman filter with input forces and control forces terms. The equations are shown as follows:

$$\hat{X}(k/k-1) = \Phi\hat{X}(k-1/k-1) + \Lambda U(k-1) + \Gamma\hat{F}(k-1), \tag{34}$$

$$P(k/k-1) = \Phi P(k-1/k-1)\Phi^{\mathrm{T}} + \Gamma Q\Gamma^{\mathrm{T}}, \tag{35}$$

$$\hat{Z}(k) = Z(k) - H[\Phi\hat{X}(k-1/k-1) + \Lambda U(k-1) + \Gamma\hat{F}(k-1)], \tag{36}$$

$$S(k) = HP(k/k-1)H^{\mathrm{T}} + R, \tag{37}$$

$$K_a(k) = P(k/k-1)H^{\mathrm{T}}S^{-1}(k), \tag{38}$$

$$P(k/k) = [I - K_a(k)H]P(k/k-1), \tag{39}$$

$$\hat{X}(k/k) = \Phi\hat{X}(k/k-1) + K_a(k)\hat{Z}(k). \tag{40}$$

The schematic diagram of the structural vibration control by the proposed method is shown in Fig. 4.

4. Numerical simulations and discussion

To verify the practicability and effectiveness of the proposed control method, numerical experiments are performed on several linear lumped-mass systems. The computational procedure for the numerical simulations is summarized as follows:

Step 1: Derive the equations of motion (Eqs. (1) or (2)) and transform them into the state equations.
Step 2: Discretize the state and measurement equations (Eqs. (9) and (10)) into the discrete-time dynamic equations (Eqs. (11) and (12)) for implementation on digital computers.
Step 3: Establish the quadratic performance index $J_i(U)$, i.e., Eq. (28), and assign the weighting matrices Q_0, Q_1, and Q_2. To simplify the interpretation of the weighting matrices, it is assumed that $Q_0 = Q_1 = Q_s \times I_{2n\times 2n}$ and $Q_2 = Q_c \times I_{2n\times 2n}$, where Q_s and Q_c denote the state and control weightings, respectively.
Step 4: Solve the Ricatti equation, i.e., Eq. (31), and evaluate the regular gain by Eq. (30) in reverse time.
Step 5: Assume the initial state of the structural system and the initial conditions of the input forces estimator and Kalman filter.
Step 6: Obtain the simulated responses at time k by solving the direct problem, i.e., Eqs. (3)–(8).
Step 7: Estimate the input disturbance forces $\hat{F}(k)$ by the input estimation approach, i.e., Eqs. (13)–(25).
Step 8: Estimate the full state vector at time k (i.e., $\hat{X}(k)$) by the Kalman filter, i.e., Eqs. (34)–(40).
Step 9: Compute the proper control force vector $U(k)$ at time k from Eq. (33).
Step 10: Repeat the above calculation process (Steps 6–9) until the final time step.

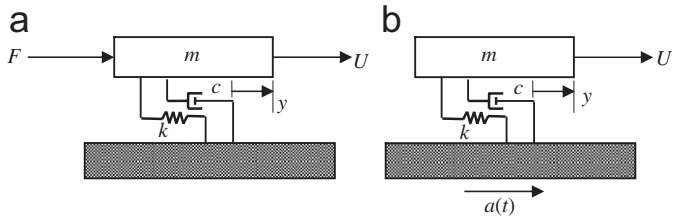

Fig. 2. A sdof lumped-mass structure (a) under force excitation and (b) under seismic excitation.

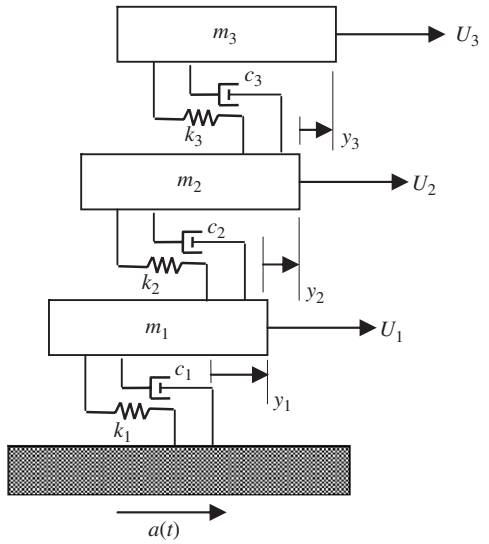

Fig. 3. A 3dof lumped-mass structure under seismic excitation.

4.1. Numerical simulation example 1

The linear sdof lumped-mass system studied by Xu and Yang [11], as shown in Fig. 2(a), is considered. The input force with rectangular, triangular, and sine configurations is given as

$$F(t)=\begin{cases} 0\ [\mathrm{N}], & 0\leqslant t\leqslant 1\ [\mathrm{s}],\\ 6000\ [\mathrm{N}], & 1<t\leqslant 2.4\ [\mathrm{s}],\\ 0\ [\mathrm{N}], & 2.4<t\leqslant 5\ [\mathrm{s}],\\ 5400\times(7-t)\ [\mathrm{N}], & 5<t\leqslant 6\ [\mathrm{s}],\\ 0\ [\mathrm{N}], & 6<t\leqslant 7\ [\mathrm{s}],\\ 6000\times\sin\left(\dfrac{8\pi}{5}(t-8)\right)\ [\mathrm{N}], & 7<t\leqslant 13.52\ [\mathrm{s}],\\ 0\ [\mathrm{N}], & 13.52<t\leqslant 15\ [\mathrm{s}]. \end{cases}$$

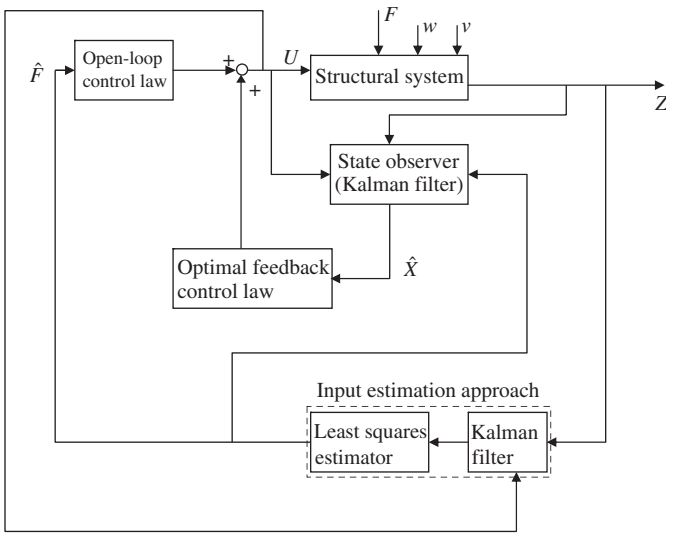

Fig. 4. Schematic diagram of the active vibration control algorithm.

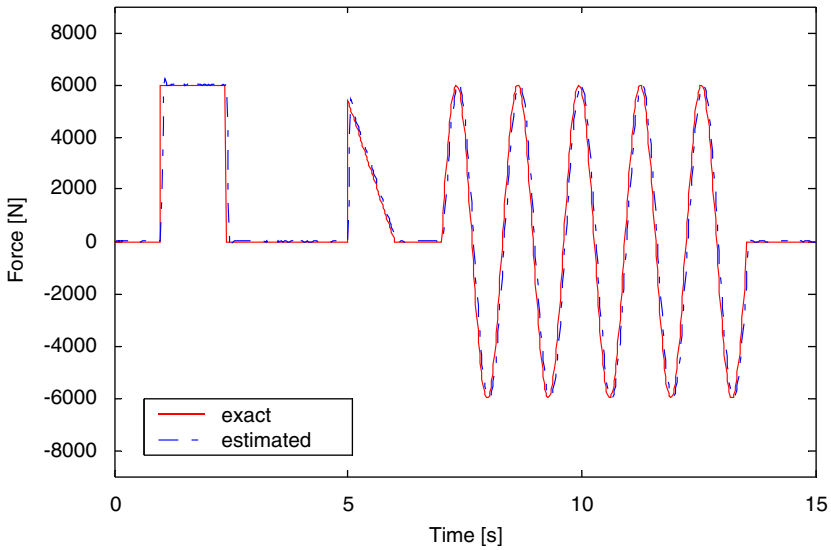

Fig. 5. Time histories of the estimated and exact input forces of the sdof lumped-mass system ($Q_s = 10^9$; $Q_c = 10^0$).

The simulation conditions and system parameters are given as the following: null initial conditions, $m = 1100\,\text{kg}$, $c = 2700\,\text{N s m}^{-1}$, $k = 43\,426\,\text{N m}^{-1}$, sampling time interval $\Delta T = 0.02\,\text{s}$, control force distribution matrix $D = 0.74 \times I_{1\times 1}$, covariance of process noise $Q = Q_w \times I_{1\times 1}$, $Q_w = 1 \times 10^1$, covariance of measurement noise $R = \sigma^2 \times I_{1\times 1}$, $\sigma = 1 \times 10^{-6}$, state weighting matrices $Q_0 = Q_1 = Q_s \times I_{1\times 1}$, $Q_s = 1 \times 10^9$, control weighting matrix $Q_2 = Q_c \times I_{1\times 1}$, $Q_c = 1$ (Figs. 3 and 4). Fig. 5 depicts the time histories of the estimated and exact input forces. The time histories of the responses of the sdof linear system with and without control are shown in Figs. 6 and 7. Fig. 8 shows the overall time histories of the control forces required for the proposed method and LQG approach.

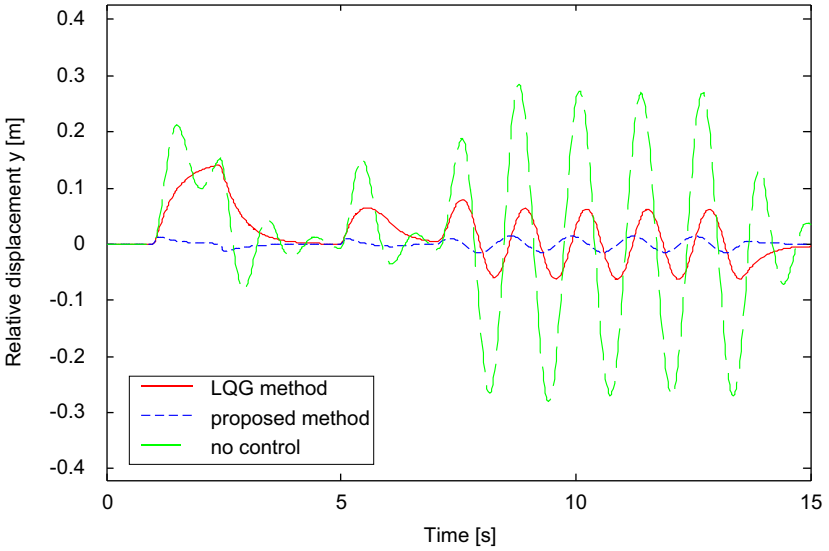

Fig. 6. Time histories of the relative displacements of the sdof lumped-mass system (force excitation; $Q_s = 10^9$; $Q_c = 10^0$).

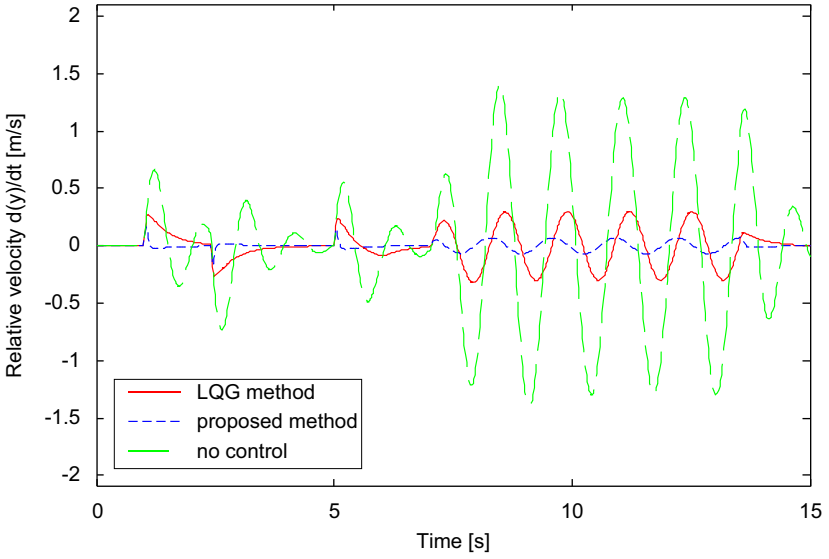

Fig. 7. Time histories of the relative velocities of the sdof lumped-mass system (force excitation; $Q_s = 10^9$; $Q_c = 10^0$).

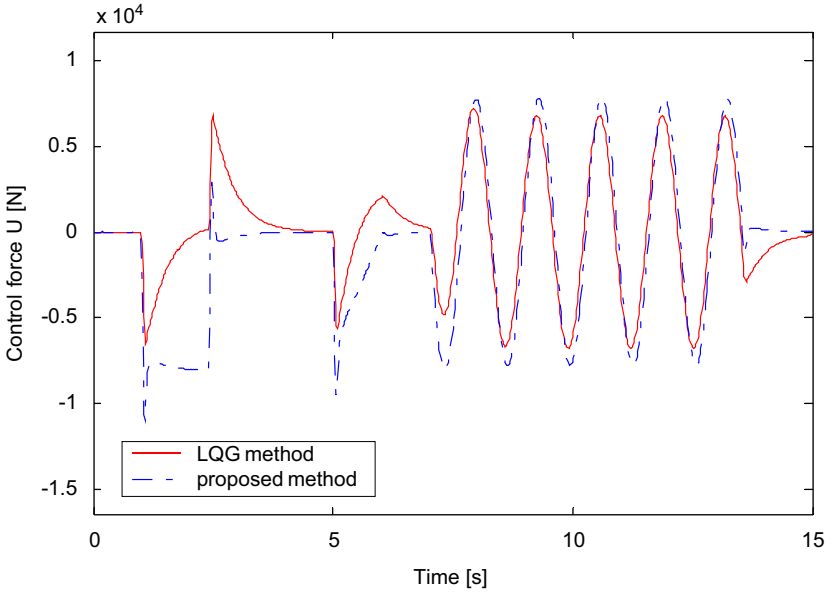

Fig. 8. Time histories of the control forces of the sdof lumped-mass system (force excitation; $Q_s = 10^9$; $Q_c = 10^0$).

Table 1
Control results of the linear sdof lumped-mass system using different weightings and control methods under the force excitation

Q_s	Q_c	Q_s/Q_c	Control method	Relative displacement, y (10^{-3} m)		Relative velocity, $\dot{y}$ (10^{-2} ms^{-1})		Control force, U (N)	
				max	rms	max	rms	max	rms
10^7	10^0	10^7	Proposed method	46.108	21.444	22.698	10.892	8723.3	4582.7
			LQG method	246.17	121.75	119.71	55.671	1378.6	640.89
			No control	284.80	135.50	140.35	63.498	0.0000	0.0000
10^9	10^0	10^9	Proposed method	15.310	7.2697	16.947	3.7092	10972	4583.5
			LQG method	140.80	50.851	31.943	15.201	7221.4	3423.8
			No control	284.79	135.49	140.33	63.498	0.0000	0.0000
10^{16}	10^0	10^{16}	Proposed method	8.3413	3.9276	15.141	2.1478	12630	4593.8
			LQG method	81.488	27.142	18.115	5.8216	10310	4027.8
			No control	284.79	135.50	140.29	63.500	0.0000	0.0000

In order to investigate the influences of the weighting matrices, we first change the state weighting from $Q_s = 10^9$ to 10^{16} and keep the value of Q_c invariant. Due to enlarge state weighting Q_s, the root mean square (RMS) and maximum values of the relative displacement of the structure controlled by the proposed method decrease to 3.9276×10^{-3} and 8.314×10^{-3} m, respectively. Next, the state weighting is adjusted from $Q_s = 10^9$ to 10^7 with fixed Q_c. The RMS and maximum of the relative displacement increase to 21.444×10^{-3} and 46.108×10^{-3} m, respectively. The control results of various weighting matrices are listed in Table 1, including the RMS relative displacement (velocity), the maximum relative displacement (velocity), the RMS control force, and the maximum control force.

4.2. Numerical simulation example 2

In the second example, the previous sdof linear system is still considered. However, the input excitation is given as the horizontal seismic ground acceleration $a(t)$, as shown in Fig. 2(b), which is the first 15 s-part of the

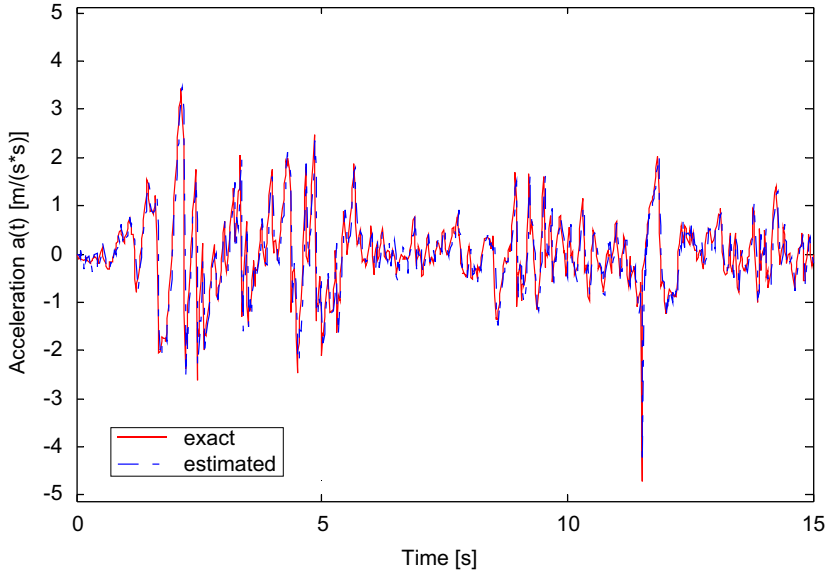

Fig. 9. Time histories of the estimated and exact base accelerations of the sdof lumped-mass system ($Q_s = 10^9$; $Q_c = 10^0$).

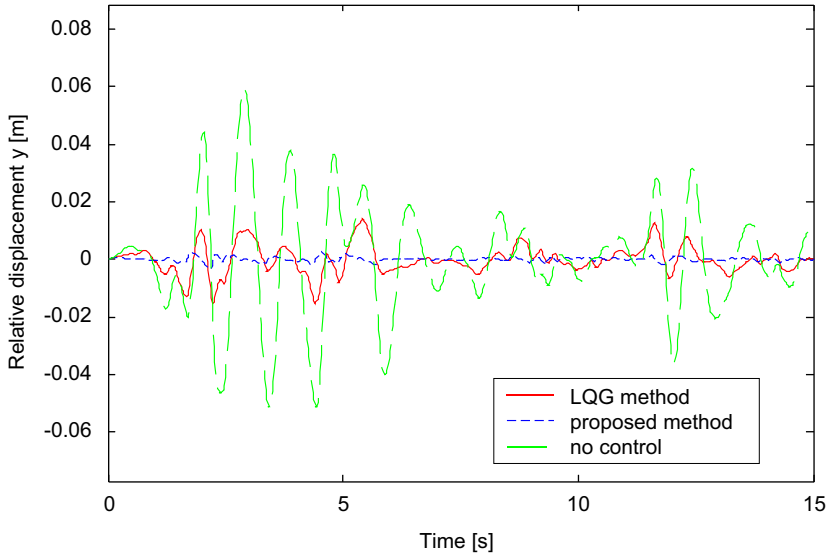

Fig. 10. Time histories of the relative displacements of the sdof lumped-mass system (seismic excitation; $Q_s = 10^9$; $Q_c = 10^0$).

North–South (NS) EI-Centro earthquake in 1940. The simulation conditions and system parameters are the same as example 1. Fig. 9 shows the time histories of the exact and estimated input accelerations. Figs. 10–12 display the time histories of the simulated responses and required control force of the sdof linear system using various control methods. The control results of the sdof structure are also summarized in Table 2.

4.3. Numerical simulation example 3

In the last example, the linear 3dof lumped-mass system studied by Xu and Yang [13], as shown in Fig. 3, is used to verify the proposed control algorithm. The parameter values of the 3dof system are

$$m_1 = 1100, \quad m_2 = 1100, \quad \text{and} \quad m_3 = 1100 \ \text{[kg]},$$

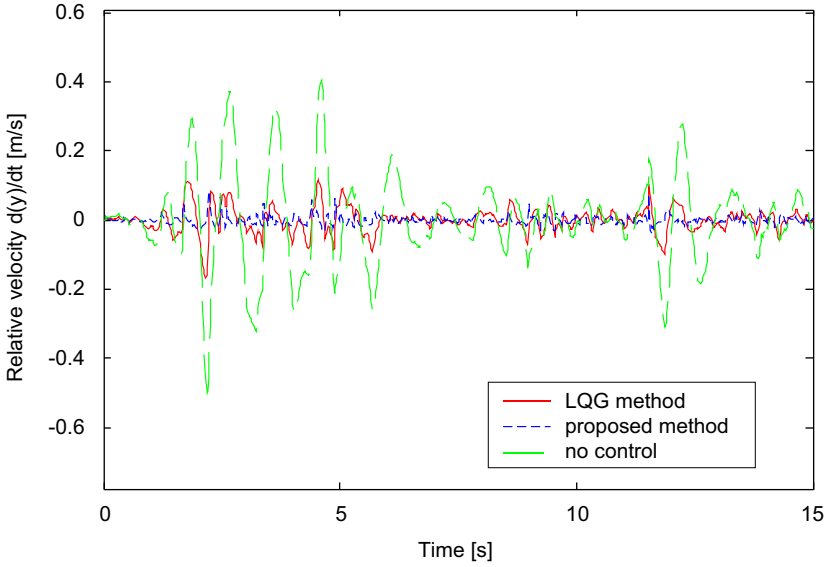

Fig. 11. Time histories of the relative velocities of the sdof lumped-mass system (seismic excitation; $Q_s = 10^9$; $Q_c = 10^0$).

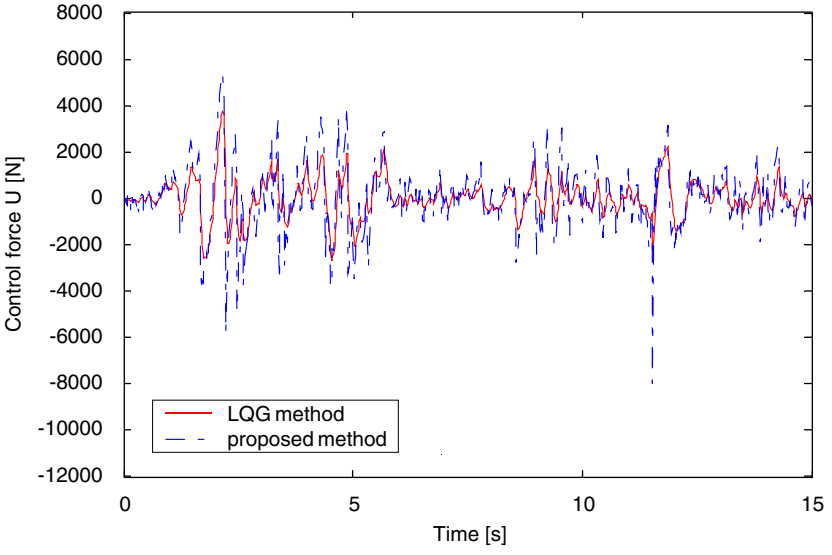

Fig. 12. Time histories of the control forces of the sdof lumped-mass system (seismic excitation; $Q_s = 10^9$; $Q_c = 10^0$).

$$c_1 = 1400, \quad c_2 = 1400, \quad \text{and} \quad c_3 = 1400 \ [\text{Ns m}^{-1}],$$

$$k_1 = 493\,300, \quad k_2 = 493\,300, \quad \text{and} \quad k_3 = 493\,300 \ [\text{N m}^{-1}].$$

The simulation conditions are taken as null initial conditions, sampling interval $\Delta T = 0.02$ s, control force distribution matrix $D = 13\,200 \times I_{3\times3}$, covariance of process noise $Q = Q_w \times I_{3\times3}$, $Q_w = 1 \times 10^{-6}$, and covariance of measurement noise $R = \sigma^2 \times I_{3\times3}$, $\sigma = 1 \times 10^{-8}$, weighting matrices $Q_0 = 10^0 \times I_{6\times6}$, $Q_1 = 10^0 \times I_{6\times6}$, $Q_2 = 1 \times I_{3\times3}$. In this numerical experiment, the first 15 s acceleration of the EI-Centro earthquake was also taken as the ground acceleration. Fig. 13 shows the time histories of the exact and estimated input accelerations. Figs. 14–16 display the time histories of the relative displacements, relative

Table 2
Control results of the linear SDOF lumped-mass system using different weightings and control methods under the seismic excitation

Q_s	Q_c	Q_s/Q_c	Control method	Relative displacement, y (10^{-3} m)		Relative velocity, $\dot{y}$ (10^{-2} ms^{-1})		Control force, U (N)	
				max	rms	max	rms	max	rms
10^7	10^0	10^7	Proposed method	9.8765	2.3184	9.9107	2.1922	6623.5	1202.8
			LQG method	47.684	16.184	47.295	11.134	547.81	129.51
			No control	57.667	19.803	51.370	12.974	0.0000	0.0000
10^9	10^0	10^9	Proposed method	1.7439	0.4354	7.5148	1.0857	9948.2	1469.7
			LQG method	8.6906	2.5998	8.9770	2.0550	4318.2	1056.3
			No control	56.336	19.018	50.961	12.971	0.0000	0.0000
10^{16}	10^0	10^{16}	Proposed method	1.3006	0.32951	8.2691	1.0453	12264	1560.5
			LQG method	6.5989	1.9496	9.2159	1.5866	6260.7	1153.7
			No control	57.700	18.986	51.044	12.933	0.0000	0.0000

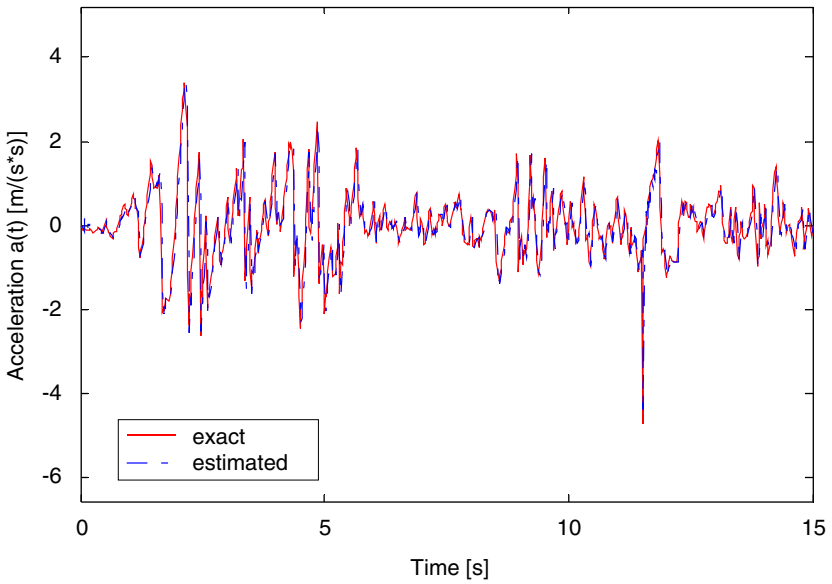

Fig. 13. Time histories of the estimated and exact base accelerations of the 3dof lumped-mass system ($Q_s = 10^9$; $Q_c = 10^0$).

velocities, and required control forces, respectively. Next, we tune the values of the state weighting Q_s to improve the control results. The state weighting matrices Q_0 and Q_1 are taken as $Q_0 = Q_1 = 10^6 \times I_{6\times6}$. The relative displacements are depicted in Fig. 17. The control results of the 3dof structural system under control with various weighting matrices are summarized in Table 3.

4.4. Discussion

(1) As illustrated in Figs. 5–17, the control effects of the proposed algorithm and LQG regulator both are obvious as long as the weighting matrices Q_0, Q_1, and Q_2 are chosen adequately. Comparing the control results, we can conclude that the proposed synthesis control method is better than the LQG regulator in vibration control.
(2) As observed from the results in Tables 1–3, we can find that the variations of Q_0, Q_1 and Q_2 will have large effects on the control performances of the LQG and proposed control methods. In general, heavy weighting matrices for responses with respect to fixed Q_2 will improve the control performances of the

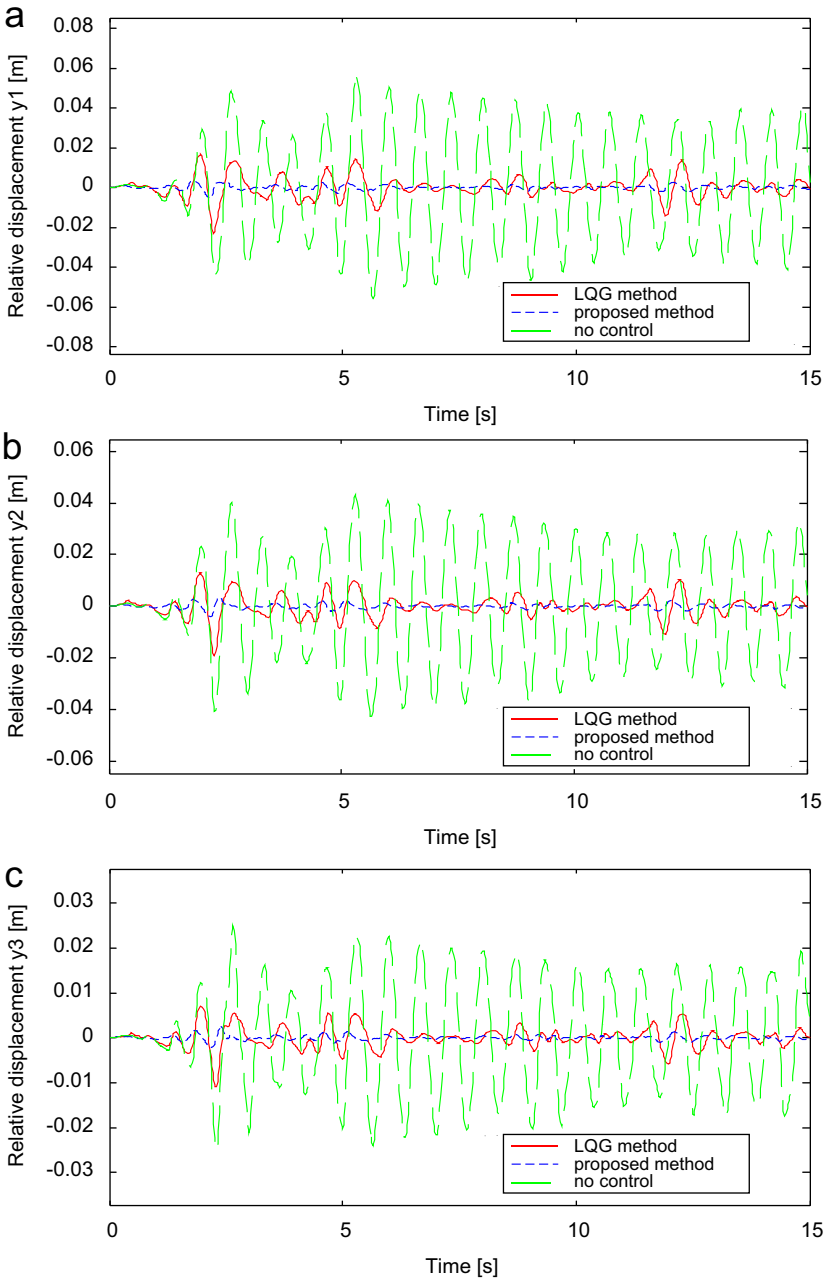

Fig. 14. Time histories of the relative displacements of the 3dof lumped-mass system: (a) y_1, (b) y_2, and (c) y_3 (seismic excitation; $Q_s = 10^9$; $Q_c = 10^0$).

LQG and proposed algorithms, but the magnitudes of the required control forces need to be increased. However, the present control method still has a better response reduction capability than that of the LQG method for various state weightings Q_s.

(3) In this study, the estimations of unmeasurable input excitations are observed from measurable states; the deficiency of ignoring unknown input disturbances can be overcome in the optimal design. Therefore, the idea of the combination of the LQG regulator and input estimation method can be applied to other fields, such as tracking problems, etc.

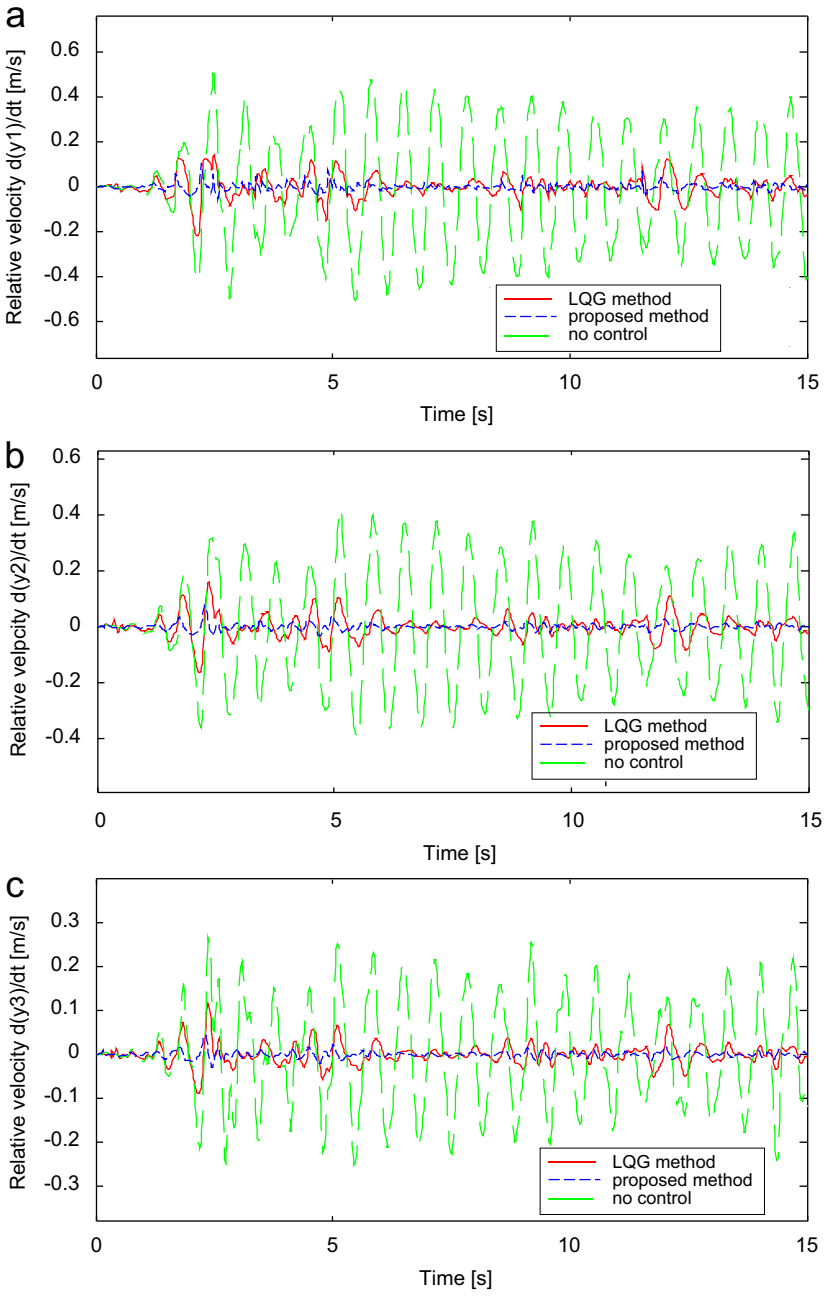

Fig. 15. Time histories of the relative velocities of the 3dof lumped-mass system: (a) $\dot{y}_1$, (b) $\dot{y}_2$, and (c) $\dot{y}_3$ (seismic excitation; $Q_s = 10^0$; $Q_c = 10^0$).

(4) Figs. 14–17 illustrate that the applicability of the present control method facilitates to suppress the vibrations of linear systems with multiple inputs and multiple outputs. Moreover, even though the synthesis control law developed in this paper is only applied to linear lumped-mass structural systems, it can readily be extended to other types of linear structural systems.

(5) In the proposed synthesis method, the control input consists of feedforward and feedback parts. The feedback part based on the LQG methodology is used to stabilize the tracking error dynamics. The LQG method with state feedback technique can provide some guaranteed robustness properties [22,23].

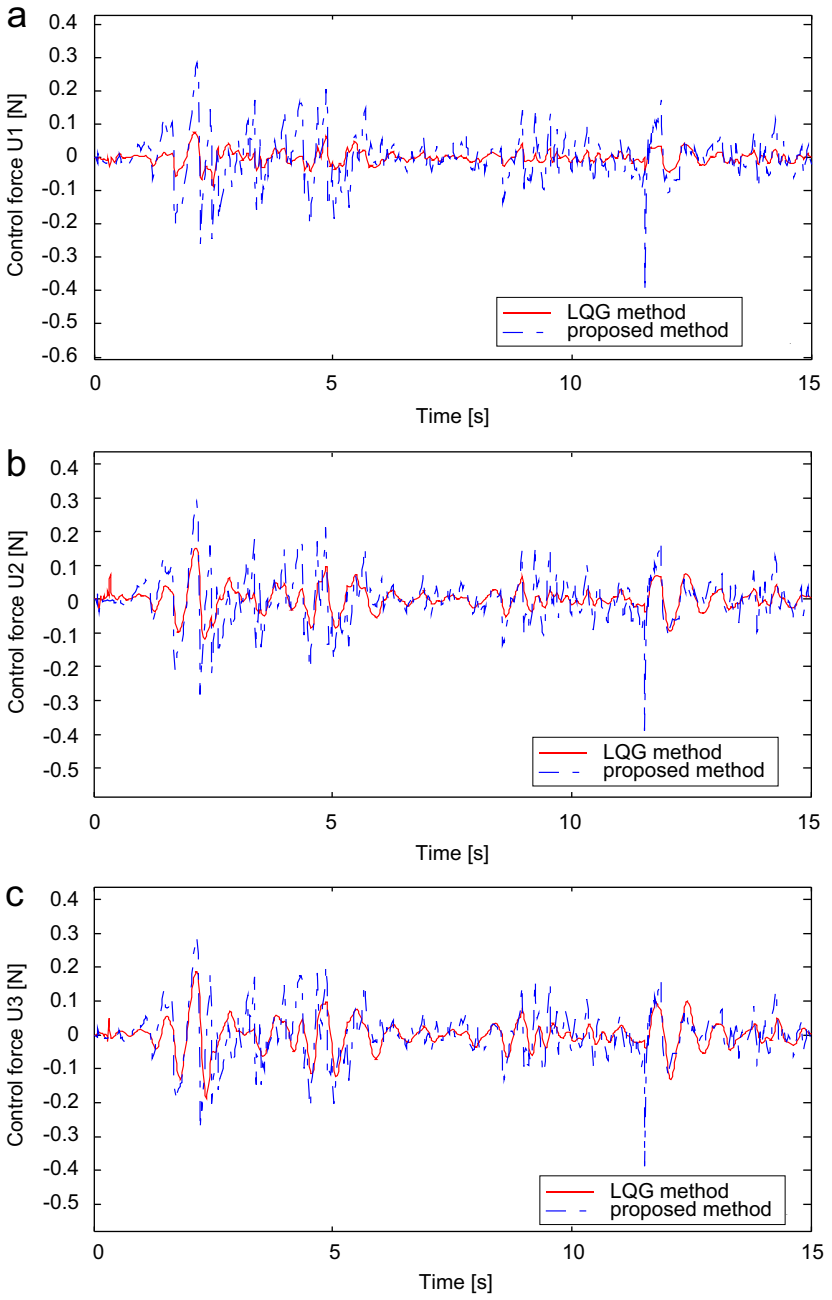

Fig. 16. Time histories of the control forces of the 3dof lumped-mass system: (a) U_1, (b) U_2, and (c) U_3 (seismic excitation; $Q_s = 10^0$; $Q_c = 10^0$).

In addition, we can incorporate the Loop Transfer Recovery (LTR) method [20] to enhance the robustness of the system, if necessary.

5. Conclusions

An active control method to suppress the vibrations of linear structural systems is presented. The control algorithm comprises two parts: the LQG regulator and the input estimation approach. The control

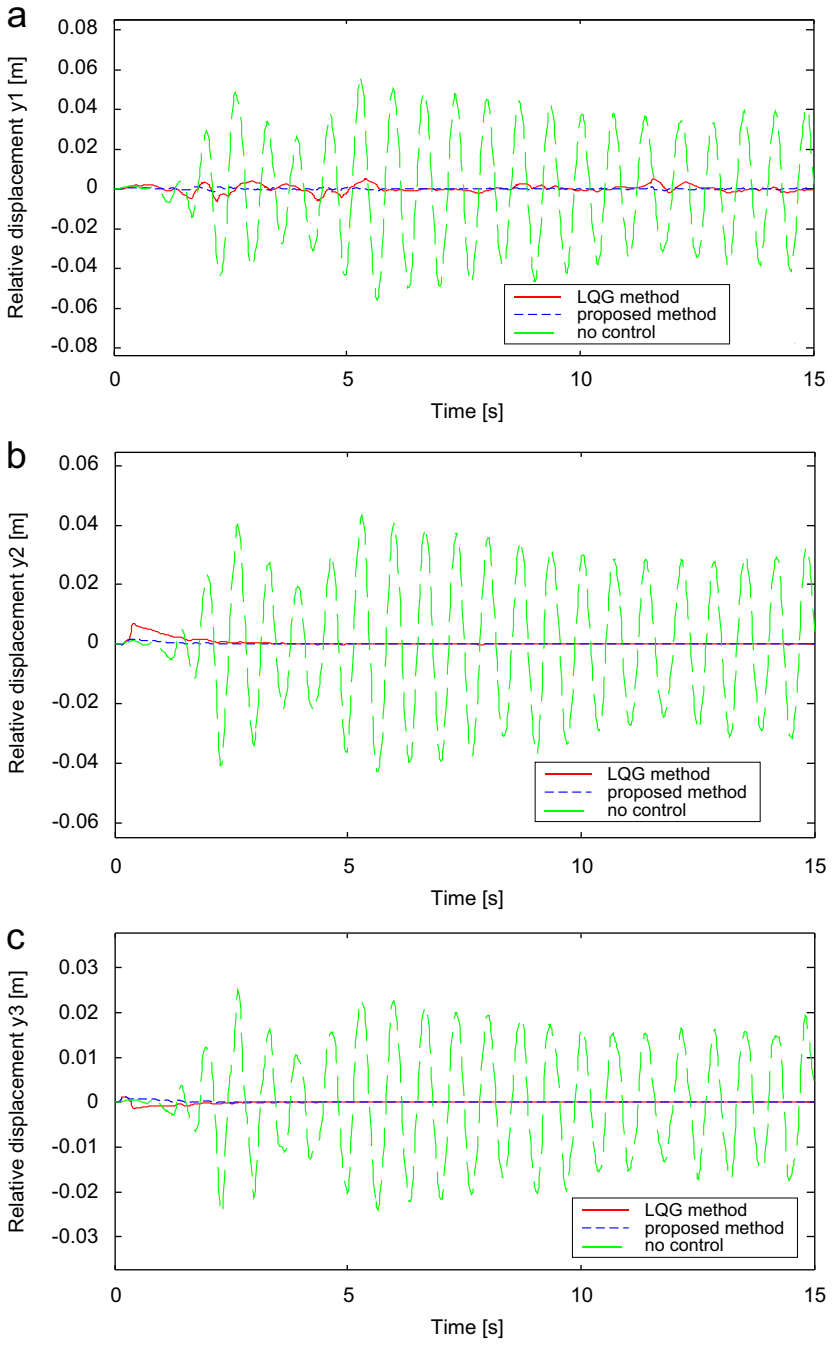

Fig. 17. Time histories of the relative displacements of the 3dof lumped-mass system: (a) y_1, (b) y_2, and (c) y_3 (seismic excitation; $Q_s = 10^6$; $Q_c = 10^0$).

performance of the proposed method is evaluated through numerical experiments of linear lumped-mass systems. The simulation results demonstrate that the proposed control method has been successfully applied to reduce the responses of structures subjected to external excitations. The vibration control performance of the present method is better than that of the conventional LQG method. The control algorithms for two and

Table 3
Control results of the linear 3DOF lumped-mass system using different weightings and control methods under the seismic excitation

State weighting Q_s	10^0			10^6		
Control weighting Q_c	10^0			10^0		
Weighting ratio Q_s/Q_c	10^0			10^6		
Control method	Proposed method	LQG method	No control	Proposed method	LQG method	No control
Relative displacement, Y (10^{-3} m)						
max						
y_1	5.1888	23.235	56.823	1.3405	6.1924	56.823
y_2	3.9948	19.251	43.149	1.6667	7.1171	43.149
y_3	2.5302	10.946	25.063	1.2435	1.5331	25.063
rms						
y_1	1.1038	5.5377	27.277	0.3568	1.8568	27.277
y_2	9.0266	4.2662	21.751	0.3349	1.2965	21.751
y_3	5.3195	2.3493	12.097	0.2033	0.3110	12.097
Relative velocity, $\dot{Y}$ (10^{-2} ms^{-1})						
max						
$\dot{y}_1$	10.756	21.880	50.722	7.8583	8.6638	50.722
$\dot{y}_2$	7.3693	16.469	41.916	2.3385	9.4380	41.916
$\dot{y}_3$	4.3591	11.542	26.557	3.8773	4.9562	26.557
rms						
$\dot{y}_1$	1.5452	5.0499	25.468	9.9785	1.5293	25.468
$\dot{y}_2$	1.1182	4.0663	20.353	0.1761	0.5756	20.353
$\dot{y}_3$	0.7354	2.3881	11.686	0.1753	0.3212	11.686
Control force, U (10^{-1} N)						
max						
U_1	4.0402	0.8538	0.0000	6.1898	4.3121	0.0000
U_2	3.8972	1.5137	0.0000	6.8476	3.6545	0.0000
U_3	3.8571	1.8662	0.0000	6.8634	3.7247	0.0000
rms						
U_1	0.6824	0.2023	0.0000	0.7628	0.9317	0.0000
U_2	0.7065	0.3665	0.0000	0.8826	0.9104	0.0000
U_3	0.7143	0.4616	0.0000	0.8807	0.7111	0.0000

three-dimensional linear structural systems are under development. Future work on this study will also include an experimental study for the proposed method.

References

[1] J.N. Yang, Application of optimal control theory to civil engineering structures, *Journal of Engineering Mechanics ASCE* 101 (1975) 818–838.
[2] L.L. Chung, A.M. Reinhorn, T.T. Soong, Experiments of active control of seismic structures, *Journal of Engineering Mechanics ASCE* 113 (1987) 1369–1386.
[3] L.L. Chung, R.C. Lin, T.T. Soong, A.M. Reinhorn, Experimental study of active control for MDOF seismic structures, *Journal of Engineering Mechanics ASCE* 113 (1987) 1369–1386.
[4] L.L. Chung, C.C. Lin, S.Y. Chu, Optimal direct output feedback of structural control, *Journal of Engineering Mechanics ASCE* 119 (1993) 2157–2173.
[5] C.C. Lin, K.H. Lu, L.L. Chung, Optimal discrete-time structural control using direct output feedback, *Engineering Structures* 18 (1996) 472–480.
[6] L.L. Chung, L.Y. Wu, T.G. Jin, Acceleration feedback control of seismic structures, *Engineering Structures* 20 (1998) 62–74.
[7] J.N. Yang, A. Akbarpour, P. Ghaemmaghami, New optimal control algorithms for structural control, *Journal of Engineering Mechanics ASCE* 113 (1987) 1369–1386.
[8] T.T. Soong, R.C. Lin, L.L. Chung, Experimental evaluation of optimal control algorithms for seismic application, *Proceedings of the ASCE Engineering Mechanics Division Sixth Specialty Conference*, at SUNY, Buffalo, NY, 1987.

[9] C.H. Loh, P.Y. Lin, N.H. Chung, Experimental verification of building control using active bracing systems, *Earthquake Engineering and Structural Dynamics* 28 (1999) 1099–1119.
[10] C.C. Chang, L.O. Yu, A simple optimal pole location technique for structural control, *Engineering Structures* 20 (1998) 792–804.
[11] N.S. Xu, Z.H. Yang, Predictive structural control based on dominant internal model approach, *Automatica* 35 (1999) 59–67.
[12] S.S. Akhiev, U. Aldemir, M. Bakioglu, Multipoint instantaneous optimal control of structures, *Computers and Structures* 80 (2002) 909–917.
[13] P.C. Tuan, C.C. Ji, L.W. Fong, W.T. Huang, An input estimation approach to on-line two dimensional inverse heat conduction problems, *Numerical Heat Transfer B* 29 (1996) 345–363.
[14] C.K. Ma, P.C. Tuan, D.C. Lin, C.S. Liu, A study of an inverse method for the estimation of impulsive loads, *International Journal of Systems Science* 29 (1998) 663–672.
[15] C.K. Ma, D.C. Lin, Input forces estimation of a cantilever beam, *Inverse Problems in Engineering* 8 (2000) 511–528.
[16] H.A. Buchholdt, *Structural Dynamics for Engineers*, Thomas Telford, 1997.
[17] R.E. Kalman, A new approach to linear filtering and prediction problem, *ASME Journal of Basic Engineering* 82 (1960) 35–45.
[18] J.M. Mendel, *Lessons in Estimation Theory for Signal Processing, Communications, and Control*, Prentice-Hall PTR, 1995.
[19] P.C. Tuan, W.T. Hou, The adaptive robust weighting input estimation method for 1-D inverse heat conduction problems, *Numerical Heat Transfer B* 34 (1998) 439–456.
[20] F.L. Lewis, V.L. Syrmos, *Optimal Control*, Wiley, New York, 1995.
[21] H. Kwakernaak, R. Sivan, *Linear Optimal Control Systems*, Wiley, New York, 1972.
[22] G.S. Michael, A. Michael, Gain and phase margin for multiloop regulators, *IEEE Transactions on Automatic Control* 22 (1977) 173–179.
[23] J.M. Lin, M.C. Lin, H.P. Wang, LEQG/LTR controller design with extended Kalman filter for sensorless brushless DC driver, *Computer Methods in Applied Mechanics and Engineering* 190 (2001) 5481–5494.